



Source apportionment of atmospheric ammonia in suburban Beijing revealed through ^{15}N -stable isotopes

Sijie Feng, Meitong Li, Kaiyan Wang, Xuejun Liu, Wen Xu^{*}

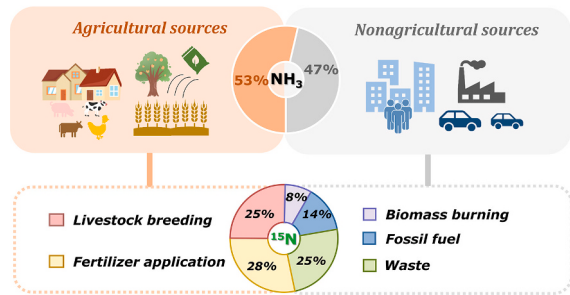
State Key Laboratory of Nutrient Use and Management, College of Resources and Environmental Sciences, National Academy of Agriculture Green Development, National Observation and Research Station of Agriculture Green Development (Quzhou, Hebei), China Agricultural University, Beijing 100193, China

HIGHLIGHTS

- Annual mean NH_3 concentrations averaged $8.7 \pm 6.9 \mu\text{g m}^{-3}$ in suburban Beijing.
- Ammonia concentrations were higher in spring and summer than in autumn and winter.
- Agricultural and non-agricultural sources contributed equally to NH_3 emissions.
- The observed atmospheric NH_3 pollution was primarily derived from local emission sources.

GRAPHICAL ABSTRACT

NH₃ emissions in suburban Beijing



ARTICLE INFO

Editor: Pavlos Kassomenos

Keywords:

Ammonia
 ^{15}N -stable isotopes
 Source apportionment
 Agricultural emissions
 Beijing City

ABSTRACT

Addressing the urgent issue of atmospheric ammonia (NH_3) emissions is crucial in combating poor air quality in megacities. Previous research has highlighted the significant contribution of nonagricultural sources, particularly fossil fuel emissions, to urban NH_3 levels. However, there is limited assessment of NH_3 dynamics in suburban areas. This study focuses on four suburban sites in Beijing, covering a 16 to 22-month observation period, to investigate spatial and temporal patterns of NH_3 concentrations. The $\delta^{15}\text{N}$ -stable isotope method is employed to identify NH_3 sources and their contributions. Our results demonstrate that agricultural sources (53 %) dominate atmospheric NH_3 emissions in suburban areas of Beijing, surpassing nonagricultural sources, and primarily emanate from local sources. Notably, fertilizer application ($37 \pm 11 \%$) and livestock breeding ($32 \pm 6 \%$) emerge as the primary contributors in summer and spring, respectively, leading to significantly elevated NH_3 concentrations during these seasons. Even in autumn and winter, both agricultural (49 %) and nonagricultural (51 %) sources contribute almost equally to NH_3 emissions. This study emphasizes the need for coordinated efforts to control atmospheric NH_3 pollution in Beijing City, with particular attention to addressing both vehicular and agricultural emissions.

* Corresponding author.

E-mail address: wenxu@cau.edu.cn (W. Xu).



1. Introduction

Ammonia (NH_3) is a significant alkaline gas present in the atmosphere, and it plays a crucial role in the formation of particulate matter (Meng et al., 2022b). This is primarily achieved by neutralizing sulfuric (H_2SO_4) and nitric acids (HNO_3) and interacting with gas-phase organic acids, resulting in the production of secondary ammonium (NH_4^+) and organic aerosols (Gunthe et al., 2021; Han et al., 2020; Pozzer et al., 2017). These interactions have implications for human health and economic costs (Giannadaki et al., 2018). Excessive NH_3 emissions and deposition can have detrimental effects on the environment, including soil acidification, eutrophication of water bodies, and biodiversity loss (Behera et al., 2013).

China, as a vast agricultural country, has emerged as a global hotspot for NH_3 emissions due to intensive anthropogenic activities over the past three decades (Liu et al., 2022; Zhang et al., 2018a). The total NH_3 emissions have been increasing at an annual rate of 1.9 % from $12.1 \pm 0.8 \text{ Tg N yr}^{-1}$ in 2000 to $15.6 \pm 0.9 \text{ Tg N yr}^{-1}$ in 2015 (Zhang et al., 2017). However, it is worth noting that China has not yet implemented an effective policy specifically aimed at controlling NH_3 emissions (Bai et al., 2019). Despite the implementation of strict policies targeting sulfur dioxide (SO_2) and nitrogen oxide (NO_x) to improve air quality since the 2010s (Xu et al., 2017, 2019), such as the Air Pollution Prevention and Control Action Plan in 2013 (SCPRC, 2013) and the Three-Year Action Plan for Winning the Blue Sky Defense Battle in 2018 (SCPRC, 2018), there has been an increase in NH_3 emission with an annual rate of 1.9 % from 2000 ($12.1 \pm 0.8 \text{ Tg N yr}^{-1}$) to 2015 ($16.6 \pm 0.9 \text{ Tg N yr}^{-1}$) (Zhang et al., 2017) due to lack of widely promotable measures as well as substantial reductions in concentrations of SO_2 and NO_x (Zheng et al., 2018; Xu et al., 2022). This increase in NH_3 concentration is now hindering the mitigation of atmospheric $\text{PM}_{2.5}$ pollution (Fu et al., 2017). Moreover, regional NH_3 -related pollution has also aggravated due to the growing disconnect between crop and livestock production systems (Zhang et al., 2019a). Even in Beijing, where rigorous measures were undertaken to control SO_2 and NO_x emissions during the 2010s, NH_3 concentrations remain among the highest globally (Pan et al., 2016). Therefore, it is critical to develop precision-targeted strategies for reducing NH_3 emissions (Meng et al., 2024; Xu et al., 2022), which requires a comprehensive analysis of NH_3 sources and their respective contributions.

Beijing is situated in the North China Plain (NCP), a region known for its intensive crop and animal production (Feng et al., 2022). As a result, it is the highest NH_3 emission region in China and is considered a global hotspot (Liu et al., 2022). Unlike other regions in Beijing-Tianjin-Hebei (BTH) area, which struggle with severe air pollution issues (Peng et al., 2024), Beijing comprises only 14 % of the total number of enterprises in the entire region (NBSC, 2021). However, as one of the largest cities in China, Beijing has a staggering number of vehicles, reaching 4.8 million with an annual growth rate of 13 % between 2005 and 2010 (Yang et al., 2014). Consequently, the interplay of agricultural and nonagricultural NH_3 emissions in Beijing has garnered great attention in recent studies, emphasizing the importance of understanding the sources of NH_3 (Chang et al., 2019; Gu et al., 2022a; Gu et al., 2022b; Zhang et al., 2020). In urban areas of Beijing, several studies have identified substantial contributions from nonagricultural sources, ranging from 62 % to 76 % (Gu et al., 2022a; Zhang et al., 2020). Moreover, differences in daily mean NH_3 mixing ratios between urban and suburban areas indicate distinct contributions from urban and suburban NH_3 sources and sinks (Lan et al., 2021). However, the quantification of NH_3 emission sources in suburban Beijing remains limited, which poses challenges for the development of targeted NH_3 control policies in the city.

Atmospheric NH_3 levels at a particular location can be influenced by a combination of local emissions and longer-range transport from other regions (Zhang et al., 2018b). Although emission inventory has been wildly used to assess NH_3 emissions and sources in specific regions, they rely on the accuracy of activity data and emission factors (Chen et al.,

2023), which still contain large uncertainties in agricultural emissions (Zhang et al., 2017; Zhou et al., 2016). To overcome these limitations, the analysis of $\delta^{15}\text{N}$ values of aerosol NH_4^+ and NH_3 has emerged as a promising and innovative approach for precisely identifying regional NH_3 sources (Chang et al., 2016; Chang et al., 2019; Feng et al., 2022; Pan et al., 2016). Several studies have successfully applied the $\delta^{15}\text{N}$ -Stable Isotope method to trace the main sources of NH_3 in various regions, including the United States (Berner and David Felix, 2020), China (Zhang et al., 2023) and megacities like Beijing (Gu et al., 2022a; Gu et al., 2022b; Zhang et al., 2020) and Shanghai (Chang et al., 2019). These studies have provided specific insights into the contributions of nonagricultural and agricultural sources to NH_3 emissions. Given the potential complexity of determining NH_3 source attribution in a system with a mix of multiple sources, the utilization of the $\delta^{15}\text{N}$ technique becomes crucial for achieving more precise quantification of NH_3 sources in Beijing.

Based on existing research and current knowledge, we conducted the collection of atmospheric NH_3 samples at four suburban sites in Beijing for a period of 16 to 22 months. The objective of this study was to investigate the spatial and temporal patterns of NH_3 concentrations and quantify seasonal contributions of NH_3 sources using the $\delta^{15}\text{N}$ -stable isotope method. This analysis not only aids in formulating targeted strategies for reducing NH_3 emissions but also plays a crucial role in substantially improving air quality in megacities.

2. Materials and methods

2.1. Site description

Four sampling sites were established in the suburban areas of Beijing, China (Fig. 1), namely PingGu (PG), ChangPing (CP), FangShan (FS) and HuaiRou (HR). These selected sites exhibit higher levels of agricultural activities, relatively sparse population distribution, and reduced traffic intensity compared to urban areas (Tables S2-S4). Meanwhile, these four suburban sampling sites are located outside of urban regions and are primarily situated in the north (HR) (416 m above sea level (m.a.s.l.)), south (FS) (251 m.a.s.l.), east (PG) (59 m.a.s.l.) and west (CP) (275 m.a.s.l.) directions of Beijing (Fig. 1b). Additional information for each site can be found in Table S1.

2.2. Sampling and chemical analysis

The ambient NH_3 concentrations were measured for two-week periods from January 2020 to November 2022 at the PG and HR sites, and from January 2020 to June 2022 at the CP and FS sites, covering all four seasons. Specifically, the sampling periods included spring (March to May), summer (June to August), autumn (September to November) and winter (December to February) from the period of 2020–2021, and spring, summer, and autumn for the period of 2021–2022. Adapted Low-Cost High Absorption Passive Samplers (ALPHA) were used to collect ambient NH_3 at a height of 1.5 m. After averaging three duplicates from each site, a total of 241 samples were collected. These samples were extracted with ultrapure water and analyzed using a continuous-flow analyzer (Seal AA3, Norderstedt, Germany), following established methods from previous research (Xu et al., 2015). The number of samples collected at each site is shown in Table S1.

We also collected atmospheric $\text{PM}_{2.5}$ samples at the China Agricultural University (CAU) (Fig. 1) to determine air concentrations of NH_4^+ , nitrate (NO_3^-) and sulfate (SO_4^{2-}) ions during the study period (from January 2020 to November 2022). A total of 93 samples were collected for each ion. The CAU site, located approximately 16.3 km northwest of the city center, represents the general background air quality of Beijing, characterized by low-rise buildings in the surrounding area (Chang et al., 2016). $\text{PM}_{2.5}$ samples were collected using medium-volume samplers (TH-150CIII, 100 L min⁻¹, Tianhong Co., Wuhan, China) with 90-mm quartz fiber filters (Whatman QM/A, Maidstone, UK). The

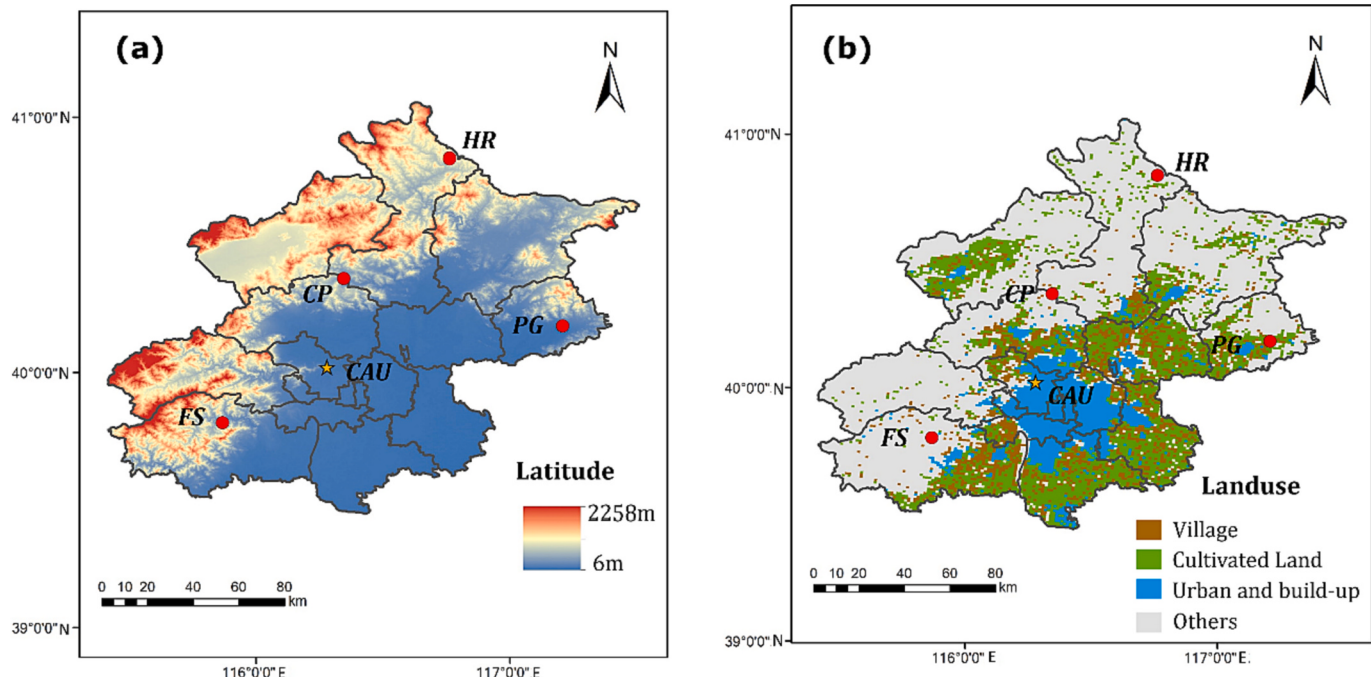


Fig. 1. Location, topography, and the land use of the sampling sites (PingGu (PG), ChangPing (CP), FangShan (FS) and HuaiRou (HR)) in Beijing City. The China Agricultural University (CAU) is the monitoring site for atmospheric PM_{2.5}. The land use type of “others” includes forests, grasslands, water bodies and wetlands (LaGro, 2005).

concentrations of cations and anions were determined using Dionex-600 and Dionex-2100 Ion Chromatographs (Dionex Inc., Sunnyvale, CA, USA), respectively. Further details of the sampling and measurements can be found in Xu et al. (2016). The concentrations of NH₄⁺, NO₃⁻, and SO₄²⁻ in the sampled PM_{2.5} are presented in Fig. S1a.

2.3. Isotopic composition analyses

The δ¹⁵N-NH₃ value was utilized to estimate the relative contribution of NH₃ emission sources to the total NH₃ emissions. We determined δ¹⁵N - NH₃ for NH₃ samples collected at four sampling sites during a two-week period throughout one year (from January 2020 to January 2021) (Table S1). The δ¹⁵N-NH₃ was measured using the hydroxylamine (NH₂OH) method at the Stable Isotope Ecology Laboratory, Institute of Applied Ecology, Chinese Academy of Sciences (Liu et al., 2014; Pan et al., 2016). The isotopic composition analyses are described in detail in Feng et al. (2022).

In this study, we considered five sources of NH₃ emissions. The agricultural sources include fertilizer application (Fa) and livestock breeding (Lb), which are widely recognized NH₃ emission sources in China (Huang et al., 2012; Kang et al., 2016; Zhang et al., 2018a). For nonagricultural sources, our analysis encompassed fossil fuel (vehicle) (Ff), waste (includes solid waste, wastewater, and human excreta) (Wa) and biomass burning (Bb). Previous studies have shown that fossil fuel (vehicle) is an important source of NH₃ emissions in Beijing (Gu et al., 2022a; Gu et al., 2022b; Zhang et al., 2020). The role of waste sources in densely populated cities has also been indicated by Chang (2014). Biomass burning is also found to be an important NH₃ emission source with the relative contributions of ~15 %–20 % (Wu et al., 2024).

To improve the accuracy of source apportionment, we utilized seasonal NH₃ isotope source profiles for fertilizer application, livestock breeding, fossil fuel (vehicle), and waste from the previous study conducted in Beijing (Tables S5 and S6) (Wang et al., 2022a). Due to a lack of seasonal data for the biomass burning profile, we referenced it from other studies (Kawashima and Kurahashi, 2011; Liu et al., 2017; Wu et al., 2019) (Table S5).

2.4. Isotope mixing model

Applying Bayesian methods to stable isotope mixing models explicitly addresses uncertainties associated with multiple sources, isotope fractionation, and isotopic signatures (Ward et al., 2011; Zong et al., 2017). This approach allows for the generation of precise probability estimates of source proportions. The Stable Isotope Analysis in R (SIAR) package employs this innovative Bayesian methodology to handle scenarios where numerous sources hinder the attainment of a unique solution, proving a range of possible source contributions. It should be noted that the model outputs offer probable solutions. SIAR has accurately estimated the contributions of individual NH₃ emission sources in an air mixture (Chang et al., 2019; Feng et al., 2022; Zhang et al., 2020). In this study, we used the siarsolomcmc4 function in SIAR to estimate the contributions of specific NH₃ emission sources in a mixture of NH₃ in air, implemented in R (3.5.3). More details about SIAR can be found in Parnell et al. (2010).

2.5. Calculation of fractionation effects

Fractionation has been defined as any process that partitions the isotopes between two substances or two phases of the same substance with different isotopic ratios. The original δ¹⁵N-NH₃ value of each sample after fractionation was calculated as follows (Berner and David Felix, 2020; Feng et al., 2022):

$$\delta^{15}\text{N-NH}_3 = (\delta^{15}\text{N-NH}_{3(o)} + \varepsilon) (f_{\text{NH}_4^+}) + (\delta^{15}\text{N-NH}_{3(o)}) (f_{\text{NH}_3}) \quad (1)$$

where:

δ¹⁵N-NH₃ is δ¹⁵N of original gas after fractionation

δ¹⁵N-NH_{3(o)} is δ¹⁵N of original gas

ε is enrichment factor

$f_{\text{NH}_4^+} = [\text{NH}_4^+]/([\text{NH}_4^+] + [\text{NH}_3])$

$f_{\text{NH}_3} = [\text{NH}_3]/([\text{NH}_4^+] + [\text{NH}_3])$

[NH₃] is NH₃ concentration measured in this study (μg m⁻³)

[NH₄⁺] is NH₄⁺ concentration measured in this study (μg m⁻³)

In this study, we considered three scenarios: the first scenario

assumes that NH_3 formation occurs exclusively via kinetic reactions ($\epsilon = -28\%$); the second assumes that NH_3 formation occurs exclusively via equilibrium exchange reactions ($\epsilon = +33\%$); and the third scenario assumes that kinetic and equilibrium reactions occur simultaneously ($\epsilon = +5\%$). To enhance the precision of our fractionation analysis and discern the contributions of NH_3 pollution sources in Beijing, we delved into the intricate mechanisms of NH_3 reactions with H_2SO_4 and HNO_3 based on one-year measurements of $\text{PM}_{2.5}$ ions in this study. Following the method of Xu et al. (2016), we calculated the molar concentrations of positive electric charges of NH_4^+ ($\text{PEC} = \text{NH}_4^+/18$) and negative electric charges of NO_3^- and SO_4^{2-} ($\text{NEC} = \text{NO}_3^-/62 + 2 \times \text{SO}_4^{2-}/96$). In cases where all sulfate was presumed to be in the form of HSO_4^- , the equation adjusted to $\text{NEC} = (\text{NO}_3^-/62 + \text{SO}_4^{2-}/96)$ (Louie et al., 2005; Zhao et al., 2013). The seasonal average PEC and NEC values are detailed in Fig. S1b.

2.6. Back trajectories, weighted potential source and weight concentration-weighted trajectory analysis

Backward trajectories arriving at each sampling site, weighted potential source contribution function (WPSCF) and weight concentration-weighted trajectory (WCWT) analysis were calculated using MeteoInfo (TrajStat package) (Wang, 2014). The trajectories were run for 24 h and initialized from a 500 m height at 3 h intervals (00:00, 03:00, 06:00, 09:00, 12:00, 15:00, 18:00 and 21:00 UTC) each day. The average NH_3 concentration was computed using the cluster statistics function.

We analyzed the potential source contribution function (PSCF) of NH_3 concentrations by integrating the average annual NH_3 concentration at each site with the backward trajectories of the air mass. The geographical region was discretized into $0.1^\circ \times 0.1^\circ$ grids. The annual averaged NH_3 concentration in each sampling site was set as the threshold (Ren et al., 2021). The PSCF value is defined as the ratio of polluted trajectory endpoints passing through the ij th grid (m_{ij}) to the total number of trajectory endpoints in the same grid (n_{ij}), denoted as (m_{ij}/n_{ij}) . To address the uncertainties associated with small n_{ij} values, WPSCF values were calculated (Ren et al., 2021; Zhang et al., 2018b). A weighting function, W_{ij} , was applied following the approach outlined by Polissar et al. (1999). Specifically, a particular W_{ij} (≤ 1.00) was multiplied if the total number of endpoints for a specific grid cell was lower than three times the average number of endpoints per grid cell. The W_{ij} was determined according to the Eq. (2) (Zhang et al., 2018b):

$$W_{ij} = \begin{cases} 1.00, & 80 < n_{ij} \\ 0.70, & 20 < n_{ij} \leq 80 \\ 0.42, & 10 < n_{ij} \leq 20 \\ 0.05, & n_{ij} \leq 10 \end{cases} \quad (2)$$

Compared to PSCF, the concentration-weighted trajectory (CWT) approach incorporates trajectory weighting based on corresponding concentrations, thereby enhancing the representation of NH_3 pollution levels along trajectories (Fleming et al., 2012). In this study, we divided the geographical domain into grid cells, with each cell covering an area of $0.1^\circ \times 0.1^\circ$. Each grid cell was assigned a residence time-weighted concentration, which was derived from the mean NH_3 concentration associated with trajectories intersecting that specific grid cell. The CWT was calculated using the Eq. (3) (Wang et al., 2022b):

$$C_{ij} = \frac{\sum_{l=1}^M C_l \tau_{ijl}}{\sum_{l=1}^M \tau_{ijl}} \quad (3)$$

where C_{ij} represents the average weighted concentration in the grid cell (ij th); C_l is the measured NH_3 concentration on the arrival of trajectory l ; τ_{ijl} is the number of trajectory endpoints in the ij th grid cell by trajectory l ; and M is the total number of trajectories.

To mitigate uncertainties, WCWT was computed by applying a

weighting function. W_{ij} , is similar to the one used in WPSCF.

2.7. Statistical analysis

A one-way analysis of variance (ANOVA) and paired-sample *t*-tests were used to assess the statistical significance of variations in mean NH_3 concentrations and $\delta^{15}\text{N}-\text{NH}_3$ for each season across all sites. The means \pm standard deviation of NH_3 concentrations and $\delta^{15}\text{N}-\text{NH}_3$ values for all sites are presented. The significance level was set at $P < 0.05$. The statistical analyses were performed using SPSS version 20.0.

3. Results and discussions

3.1. Temporal and spatial variations in ambient NH_3 concentrations

The time-averaged atmospheric NH_3 concentrations across four sites ranged from 0.7 to $50.0 \mu\text{g m}^{-3}$, with a mean value of $8.7 \pm 6.9 \mu\text{g m}^{-3}$ (241 samples) (Fig. 2). By comparing results with previous studies (Table S7), the NH_3 concentration we measured in suburban Beijing was similar to the levels observed in urban Beijing in 2014 ($9.9 \mu\text{g m}^{-3}$) (Chang et al., 2016). However, it was lower than the measurements reported by Gu et al. (2022a) for urban Beijing from September 2020 to August 2021 ($15.0 \mu\text{g m}^{-3}$) and by Lan et al. (2021) from January 2018 to January 2019 ($15.7 \mu\text{g m}^{-3}$) in suburban Beijing. Relatively higher NH_3 levels in urban areas compared to suburban regions are not exclusive to this study and have been observed in other megacities like Shanghai (Chang et al., 2019), Beijing (Meng et al., 2011) and Hong Kong (Tanner, 2007) within China, as well as in various international locations like Canada (Hu et al., 2014). The difference between urban and suburban areas can be attributed to the significant impact of nonagricultural NH_3 emissions from intense traffic (Chang et al., 2019; Gu et al., 2022b). However, in comparison to suburban areas in other major Chinese cities, our findings were higher than those in the Chinese Megacity- Shanghai ($5.5 \mu\text{g m}^{-3}$) (Chang et al., 2015). This disparity may be related to differences in location, soil properties, and meteorological conditions. Beijing, situated in the NCP, is a region characterized by intense crop and animal production. It features alkaline soils with higher pH levels than the southern parts of China, which promotes NH_3 loss (Chang et al., 2019). Meanwhile, Beijing's lower precipitation results in less removal of atmospheric NH_3 through wet deposition compared to Shanghai (Lan et al., 2021).

In all sites, the averaged atmospheric NH_3 concentrations in suburban Beijing exhibited variations across seasons. Specifically, NH_3 concentrations were significantly ($P < 0.05$) higher during summer ($11.9 \pm 7.7 \mu\text{g m}^{-3}$) and spring ($10.7 \pm 5.4 \mu\text{g m}^{-3}$) compared to autumn ($6.5 \pm 7.6 \mu\text{g m}^{-3}$) and winter ($5.5 \pm 4.5 \mu\text{g m}^{-3}$) (Fig. 2a). These seasonal patterns were consistently observed at each sampling site (Fig. 2b) and have been reported in previous studies conducted in Beijing (Lan et al., 2021) and other agricultural regions (Chang et al., 2019; Feng et al., 2022). Temperature plays a key role in driving NH_3 emissions from volatility-driven sources, resulting in seasonal fluctuations in NH_3 emissions (Christensen et al., 1991; Kang et al., 2016). We found that there was a significant positive correlation ($P < 0.01$) between temperature and NH_3 concentrations across the sampling periods (Fig. S2a). Based on surveys from our prior study in the NCP (Feng et al., 2022), there is intensive fertilization application for maize, wheat and fruit during spring and summer (Table S8). The volatilization of N fertilizers can cause an increase in atmospheric NH_3 (Huang et al., 2016), especially in high temperatures in summer and spring (Fig. S2b). When comparing different sites, the HR site exhibited an annual average NH_3 concentration of $4.2 \pm 2.9 \mu\text{g m}^{-3}$ ($n = 67$), significantly ($P < 0.05$) lower than that observed in the PG ($n = 62$, $11.1 \pm 7.8 \mu\text{g m}^{-3}$ on average), CP ($n = 55$, $10.5 \pm 4.6 \mu\text{g m}^{-3}$ on average), and FS ($n = 57$, $9.9 \pm 8.4 \mu\text{g m}^{-3}$ on average) sites (Fig. 2c). This pattern is also consistent across different seasons. The observed differences may be related to the complexity of suburban NH_3 sources, encompassing both agricultural

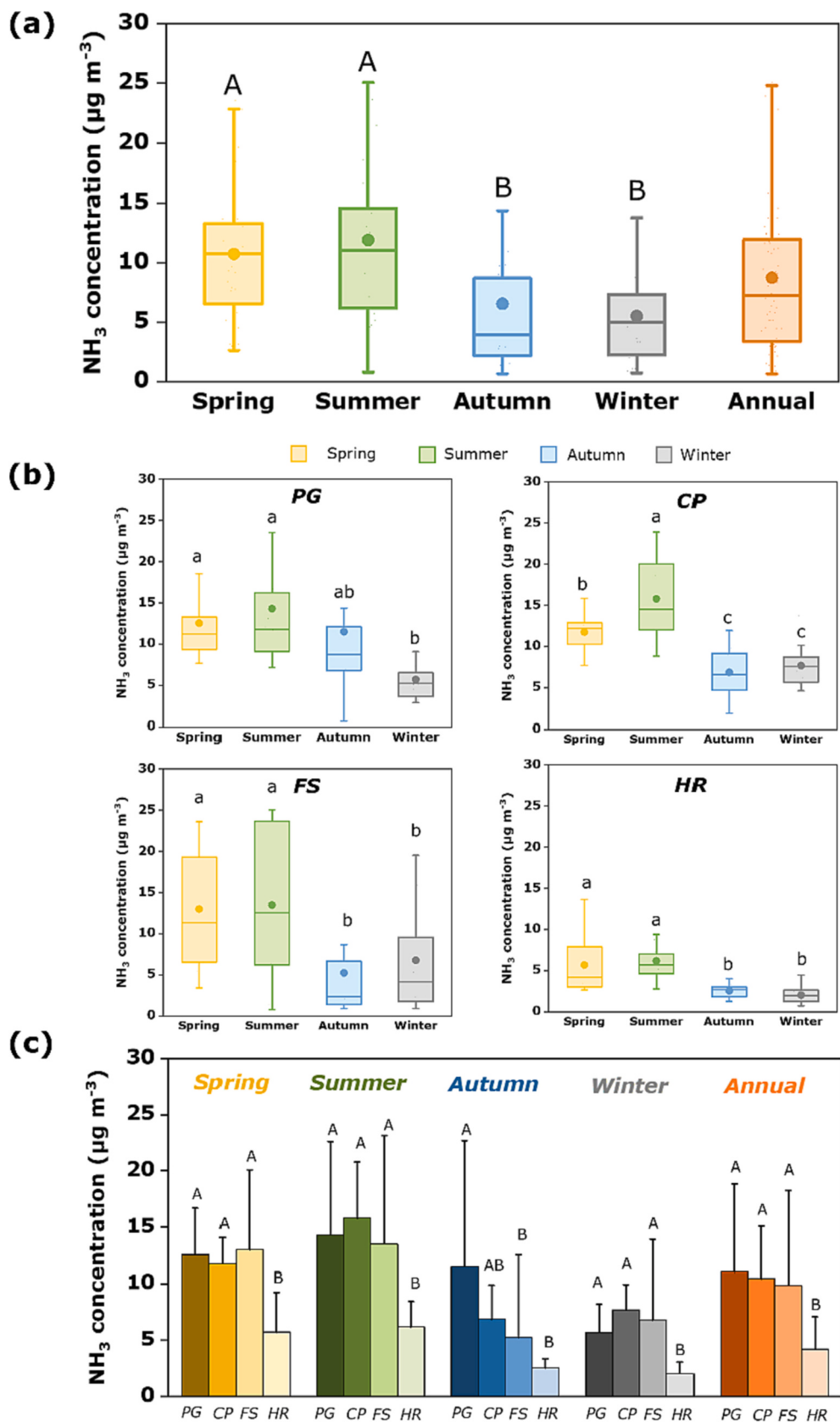


Fig. 2. (a) Mean seasonal (spring/summer/autumn/winter) and annual ammonia (NH₃) concentrations across all sampling sites. (b) Mean seasonal NH₃ concentrations in each sampling site (PingGu (PG), ChangPing (CP), FangShan (FS) and HuaiRou (HR)). (c) Comparisons of seasonal and annual mean NH₃ concentrations at the four sample sites (PG, CP, FS, HR). The upper and lower boundaries of the boxes represent the 75th and 25th percentiles; the whiskers above and below the boxes represent the 90th and 10th percentiles; the line and points within the box represent the median and mean values, respectively. Bars with different letters denote significant differences between sites or seasons ($P < 0.05$) (uppercase and lowercase letters represent different sites and different seasons, respectively).

and non-agricultural activities. Specifically, HR exhibits a relatively low population density and minimal agricultural activities compared to other sampling sites (Tables S2-S4).

3.2. Isotopic characteristics of atmospheric NH₃

N naturally occurs in two stable isotopes, ¹⁴N and ¹⁵N. The slight mass difference between them leads to variations in the physicochemical behavior of molecules. This results in different ratios of ¹⁵N to ¹⁴N, expressed as δ¹⁵N-NH₃ (‰). Therefore, the δ¹⁵N-NH₃ value was utilized to determine the fraction of total NH₃ attributed to each NH₃ emission source (Berner and David Felix, 2020; Chang et al., 2019). Throughout the study period, the annual mean δ¹⁵N-NH₃ values (‰) for all sites was -35.5 ± 7.6 ‰, ranging from -21.9 ‰ to -62.8 ‰. Specially, the annual mean δ¹⁵N-NH₃ value for PG ($n = 23$), CP ($n = 22$), FS ($n = 21$) and HR ($n = 18$) sites were -35.6 ± 9.2 ‰, -33.8 ± 6.1 ‰, -35.6 ± 7.5 ‰ and -37.5 ± 7.1 ‰, respectively, without significant differences observed among all sites (Table S9). In comparison with other studies shown in Table S7, our findings indicated lower δ¹⁵N-NH₃ values than those measured in urban regions of Beijing such as Gu et al. (2022a) (-17.5 ± 3.8 ‰) and Gu et al. (2022b) (-24.9 ‰), which reported higher contributions from nonagricultural sources. The consistently low

δ¹⁵N-NH₃ values observed in our ambient NH₃ samples suggest a connection to agricultural activities (Berner and David Felix, 2020). Similar values have been observed in rural areas within the NCP (Feng et al., 2022) and Shanghai (Chang et al., 2019). Additionally, when comparing the agricultural data between urban and suburban areas of Beijing (Table S3 and Table S4), it is evident that the suburban areas have a significantly higher proportion of crop production (96 %–100 %) and animal production (98 %–100 %), highlighting the substantial influence of agricultural practices in these regions. However, our δ¹⁵N-NH₃ values also align closely with findings from studies conducted in urban Beijing (Chang et al., 2016; Zhang et al., 2020), which indicated that non-agricultural sources contribute to nearly half of the NH₃ emissions. Considering the high number of vehicles and population in suburban areas of Beijing (Table S2), it is clear that non-agricultural sources also play a non-negligible role in NH₃ contributions in suburban regions. A comprehensive discussion on the sources of NH₃ emissions will be provided in chapter 3.3.

Across all sites, the seasonal mean δ¹⁵N-NH₃ values exhibited variations in spring, summer, autumn, and winter, averaging at -33.3 ± 4.9 ‰, -33.3 ± 4.0 ‰, -39.7 ± 9.7 ‰, and -36.1 ± 8.8 ‰, respectively. Notably, the δ¹⁵N-NH₃ values were significantly ($P < 0.05$) lowest during the autumn period compared to the other seasons (Fig. 3a). This

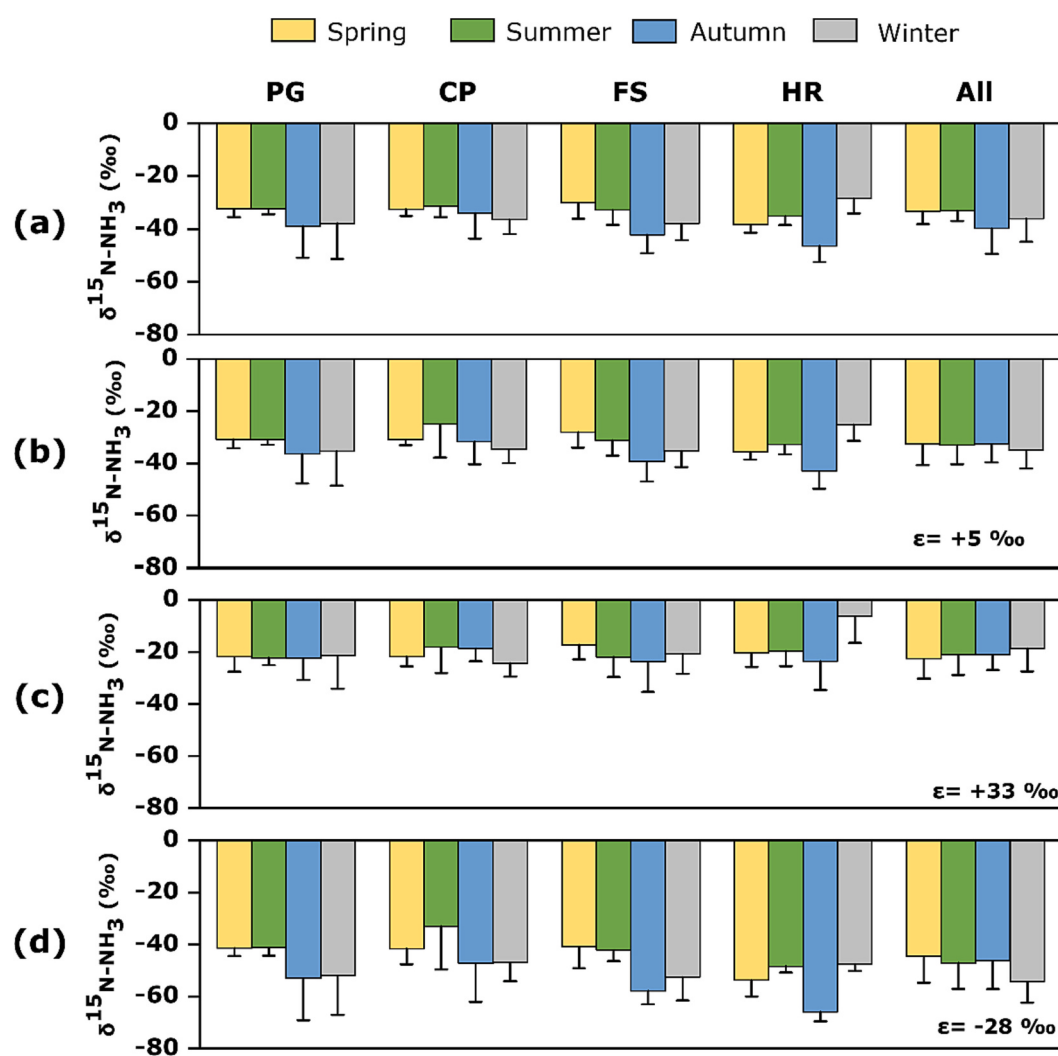


Fig. 3. δ¹⁵N-NH₃ values (‰) in each season (spring/summer/autumn/winter) in four sampling sites (PingGu (PG), ChangPing (CP), FangShan (FS) and HuaiRou (HR)) under (a) original, (b) ε = +5 ‰ fractionation scenario (NH₃ formation occurred via kinetic and equilibrium reactions simultaneously), (c) ε = +33 ‰ fractionation scenario (NH₃ formation occurred exclusively via equilibrium exchange reactions) and (d) ε = -28 ‰ fractionation scenario (NH₃ formation occurred exclusively via kinetic reactions).

seasonal pattern of $\delta^{15}\text{N-NH}_3$ values is distinct from the observed variation in NH_3 concentration described in chapter 3.1. Furthermore, we did not identify a significant relationship between $\delta^{15}\text{N-NH}_3$ values and temperature. Therefore, it is reasonable to assume that the different $\delta^{15}\text{N-NH}_3$ values are mainly related to the emission sources (Zhang et al., 2020). Notably, the $\delta^{15}\text{N-NH}_3$ values during spring, summer, and autumn closely resembled the $\delta^{15}\text{N-NH}_3$ profile associated with N-fertilizer application in the corresponding seasons (spring: -32.2‰ ; summer: -35.6‰ ; and autumn: -39.5‰) (Table S5). Analysis of N fertilization activities revealed intensive fertilization application for maize, wheat, and fruit during spring and summer, while baseline fertilization practices for wheat and organic fertilization of fruit were observed during the autumn season (Table S8). Information from the Beijing Statistic Yearbook (Table S3) further supported these findings, indicating that the suburban areas surrounding Beijing were involved in full-scale maize, wheat, and fruit production. This intensive crop production offers a compelling explanation for the lowest $\delta^{15}\text{N-NH}_3$ values observed during these seasons.

Nevertheless, it is imperative to acknowledge that the $\delta^{15}\text{N-NH}_3$ values from sources can undergo alterations due to various fractionation processes during emission, necessitating careful consideration when analyzing the stable isotope composition of ambient samples. In light of this, our study takes into account three distinct scenarios ($\varepsilon = -28\text{‰}$, $\varepsilon = +33\text{‰}$, and $\varepsilon = +5\text{‰}$) for NH_3 fractionation (Fig. 3b, c, d) (Berner and David Felix, 2020). We found that there was ample NH_4^+ to form ammonia bisulfate (NH_4HSO_4) in most seasons, although it was insufficient for the complete neutralization of SO_4^{2-} and NO_3^- necessary for the formation of ammonium sulfate ($(\text{NH}_4)_2\text{SO}_4$) aerosols (Fig. S1b). This indicated that during the sampling periods, Beijing was under acidic conditions. Consequently, the kinetic and equilibrium reactions will occur simultaneously, we employed the scenario with $\varepsilon = +5\text{‰}$ (Berner and David Felix, 2020) to apportion the sources of NH_3 in the subsequent sections, aligning our analysis with the prevailing acidic conditions observed in the region.

3.3. Source contributions of ambient NH_3

Fig. 4 illustrates the distribution of emission sources among the four sites, which was determined using fractional $\delta^{15}\text{N-NH}_3$ values within the

$\varepsilon = +5\text{‰}$ scenario of the isotope mixing model. Throughout the entire sampling period, agricultural sources, including fertilizer application and livestock breeding, were found to be the predominant contributors, accounting for 53 % of the total emissions across all sites. Nonagricultural sources (including fossil fuels, waste, and biomass burning) made up the remaining 47 % (Fig. S3). Specifically, fertilizer application accounted for an average of 28 % of emissions, followed closely by livestock breeding at 25 %. Waste contributed 25 %, while fossil fuel emissions accounted for 14 %. Biomass burning had the smallest contribution, representing just 8 % of the overall emissions (Fig. S3). Similar high contributions from agricultural sources were observed in rural areas of agricultural counties in the NCP (Feng et al., 2022) and in urban Beijing (Chang et al., 2016).

In our study, the seasonal analysis revealed distinct primary contributors to NH_3 emissions: Fertilizer application accounted for $37 \pm 11\text{‰}$ of emissions in summer, while livestock breeding accounted for $32 \pm 6\text{‰}$ in spring (Fig. 4a). These findings are consistent with the high NH_3 concentrations typically observed during these seasons. The fertilizer application contribution of NH_3 emissions in spring is much higher than that measured in March in urban Beijing (11 % ~ 13 %) (Gu et al., 2022a). The PG site exhibits a high contribution (48 %) from fertilizer application during summer (Fig. 4b) due to a combination of intensive fertilization practices (Table S3), elevated temperatures (Dewes, 2009), and the mechanisms that allow the persistence of HNO_3 and NH_3 in the gas phase (Seinfeld, 2006). These conditions create an environment conducive to relatively high NH_3 concentrations observed at PG site (Fig. 2b). Additionally, in the PG, CP, and HR sites, livestock breeding accounted for over 30 % of NH_3 emissions during the spring season. This can be attributed to the production of pigs, dairy cattle, and beef cattle in the three sites (Table S4). These animals are known to have high NH_3 emission factors during housing and manure storage, compared to other livestock species, making up from 17 % to 25 % of NH_3 emissions in animal production of housing and storage systems (Ma et al., 2010; Meng et al., 2022a).

During autumn and winter, comparable contributions were made by both agricultural and nonagricultural sources, accounting for 49 % and 51 % of NH_3 emissions, respectively. Specifically, fertilizer application emerged as the dominant source, significantly contributing to ambient NH_3 levels during autumn ($26 \pm 1\text{‰}$). Among nonagricultural sources,

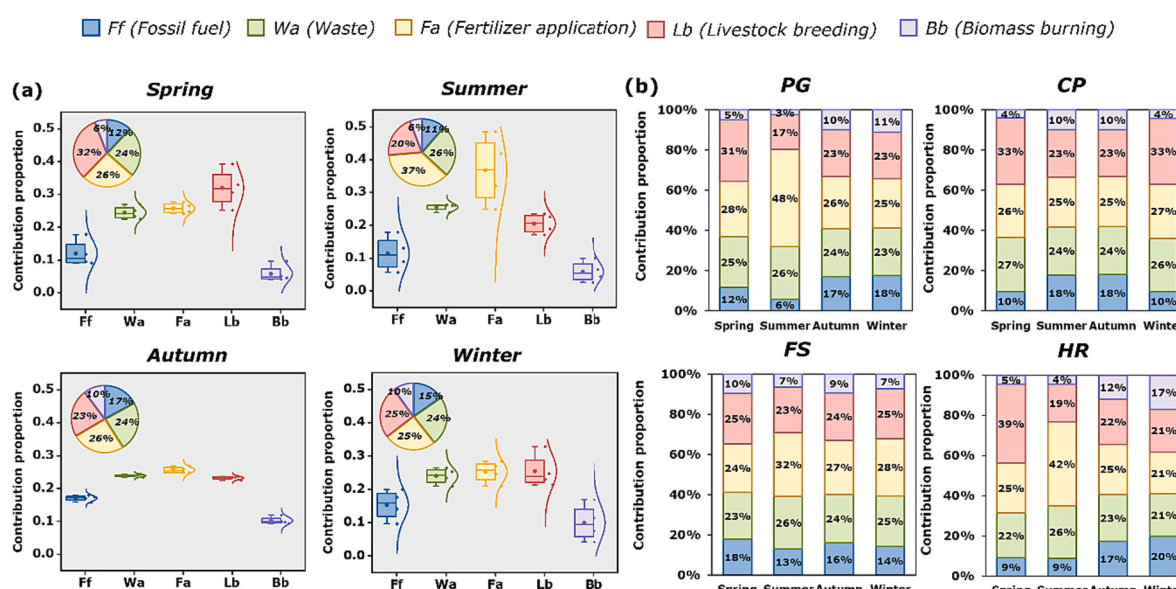


Fig. 4. (a) Seasonal normal distributions and variations (within the 5th and 95th percentiles) of agricultural (fertilizer application (Fa) and livestock breeding (Bb)) NH_3 sources at four sampling sites. (b) Relative contributions of different emission sources to atmospheric NH_3 at each sampling site (PingGu (PG), ChangPing (CP), FangShan (FS) and HuaiRou (HR)). Relative contributions were calculated using the IsoError mixing model in the $\varepsilon = +5\text{‰}$ fractionation scenario (NH_3 formation occurred exclusively via kinetic reactions).

waste made consistent contributions across all seasons, accounting for $24 \pm 4\%$, $26 \pm 1\%$, $24 \pm 0\%$, and $24 \pm 2\%$ in spring, summer, autumn, and winter, respectively. Fossil fuel emissions played a more substantial role in autumn ($17 \pm 1\%$) and winter ($15 \pm 5\%$) compared to spring ($12 \pm 4\%$) and summer ($11 \pm 5\%$). It is worth mentioning that despite vehicle emissions as the primary contributor ($21\% \sim 25\%$) in urban Beijing (Gu et al., 2022a), especially during colder seasons (Gu et al., 2022b) our results highlight the significance of agricultural activities in NH_3 emissions in the suburban area in autumn and winter.

To investigate the connection between air transport and NH_3 concentrations in potential source regions, we conducted an analysis using annual air mass back trajectories (Fig. 5a), WPSCF (Fig. 5b) and WCWT (Fig. 5c) of atmospheric NH_3 concentrations at each sampling site. The daytime backward trajectories within 500 m of the surface were categorized into five clusters, covering the entire year of 2020. We found that, although there was long-range transport from the north direction of Mongolia, PG, CP and HR sites were mainly affected by the short air masses from the southeast direction of Beijing, accounting for approximately 40 % of all trajectories for each site. Additionally, the FS site also experienced influences from the southwest of Hebei province (Fig. 5a). Further analysis of WPSCF and WCWT values indicated that while the FS site was partially influenced by the surrounding region, such as the northwest direction, the high WPSCF and WCWT values of PG, CP and

HR were primarily clustered around the respective sampling sites (Fig. 5b and Fig. 5c). These findings suggest that the main sources of NH_3 emissions are mainly from local sources. Considering a 53 % contribution of NH_3 emissions from agricultural sources (Fig. 4), it becomes imperative to tailor NH_3 emission control measures to address the significant impact of intensive agricultural activities in these suburban areas.

4. Conclusions and implications

This study presented atmospheric NH_3 levels and emission sources in four suburban sites in Beijing based on field measurements over a period of 16–22 months. Our results revealed that agricultural activities are the primary contributors to total NH_3 emissions in suburban Beijing (53 %). Particularly noteworthy is the significant role played by fertilizer application and livestock breeding, accounting for $37 \pm 11\%$ and $32 \pm 6\%$ of the total NH_3 emissions during the summer and spring, respectively. Meanwhile, analysis of air mass back trajectories, WPSCF and WCWT of atmospheric NH_3 concentrations confirm that ambient NH_3 at the four sites mainly originated from local emissions. These findings provide comprehensive perspectives for the analysis of NH_3 pollution sources in Beijing.

China has witnessed a remarkable surge in the production and sales

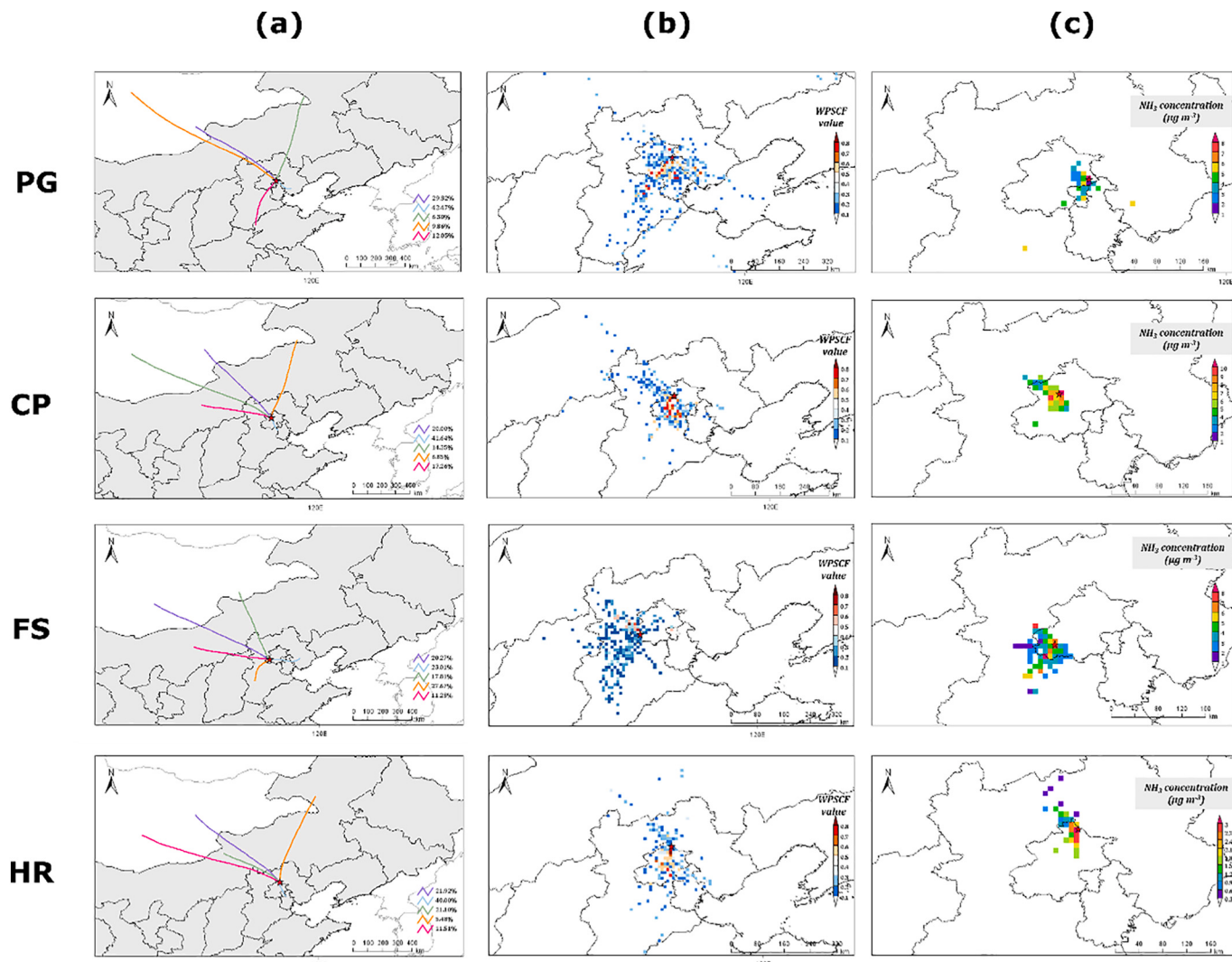


Fig. 5. (a) The maps of (a) backward trajectories of air masses, (b) weighted potential source contribution analysis (WPSCF) of atmospheric NH_3 , and (c) weighted concentration-weighted trajectory (WCWT) for four sampling sites (PingGu (PG), ChangPing (CP), FangShan (FS) and HuaiRou (HR)) of suburban Beijing from January 2020 to January 2021. The different colors indicate different clusters of backward trajectories.

of new energy vehicles (Zhang et al., 2019b), due to stringent fuel-efficiency standards for light-duty vehicles and the widespread promotion of electric vehicles since the early 2010s (Wang et al., 2014). It is worth noting that previous studies have reported that nonagricultural sources, particularly fossil fuel contributions from vehicle emissions, dominate atmospheric NH₃ pollution in urban areas of Beijing, rather than agricultural sources (Pan et al., 2016; Zhang et al., 2020). However, our findings reveal that the contribution of NH₃ emissions from agricultural and non-agricultural sources is approximately equal. Currently, Beijing, leads the nation in the total number of pure electric vehicles (Zhang et al., 2019b). Consequently, the contribution of nonagricultural sources, especially fossil fuels, to NH₃ emissions is expected to decline significantly in the coming years. This shift underscores the increasing importance of addressing agricultural sources in the context of NH₃ emissions in Beijing.

It is imperative to focus our efforts on enhancing agricultural management practices in suburban areas, with particular emphasis on optimizing crop production fertilization techniques and improving manure management for animals with high NH₃ emission factors, such as pigs, dairy cattle, and beef cattle. Implementing a combination of strategic measures such as reducing the proportion of basal nitrogen fertilizers, adopting deep placement of nitrogen fertilizers, avoiding over-fertilization (Chen et al., 2011), and integrating enhanced-efficiency fertilizers (Ju and Zhang, 2017) can prove instrumental (Kang et al., 2023). Additionally, implementing low-protein feed in animal breeding (Hou et al., 2016), and adopting techniques like covering solid and slurry manure (Mohankumar Sajeev et al., 2018), can further contribute to effectively mitigating NH₃ emissions in Beijing.

CRediT authorship contribution statement

Sijie Feng: Writing – review & editing, Writing – original draft, Visualization, Investigation, Formal analysis, Data curation. **Meitong Li:** Visualization, Investigation, Data curation. **Kaiyan Wang:** Visualization, Investigation, Data curation. **Xuejun Liu:** Writing – review & editing, Writing – original draft. **Wen Xu:** Writing – review & editing, Writing – original draft, Visualization, Supervision, Investigation, Formal analysis, Data curation, Conceptualization.

Declaration of competing interest

The authors declare that they have no known competing financial interests or personal relationships that could have appeared to influence the work reported in this paper.

Data availability

Data will be made available on request.

Acknowledgement

This study was supported by the National Natural Science Foundation of China (42175137), the China Postdoctoral Science Foundation (2019T120156 and 2018M641531), the China Scholarship Council (201913043), and the High-level Team Project of China Agricultural University.

Appendix A. Supplementary data

Supplementary data to this article can be found online at <https://doi.org/10.1016/j.scitotenv.2024.170728>.

References

- Bai, Z., Winiwarter, W., Klimont, Z., Velthof, G., Misselbrook, T., Zhao, Z., Jin, X., Oenema, O., Hu, C., Ma, L., 2019. Further improvement of air quality in China needs clear ammonia mitigation target. *Environ. Sci. Technol.* 53, 10542–10544.
- Behera, S.N., Sharma, M., Aneja, V.P., Balasubramanian, R., 2013. Ammonia in the atmosphere: a review on emission sources, atmospheric chemistry and deposition on terrestrial bodies. *Environ. Sci. Pollut. Res.* 20, 8092–8131.
- Berner, A.H., David Felix, J., 2020. Investigating ammonia emissions in a coastal urban airshed using stable isotope techniques. *Sci. Total Environ.* 707, 134952.
- Chang, Y.H., 2014. Non-agricultural ammonia emissions in urban China. *Atmos. Chem. Phys. Discuss.* 2014, 8495–8531.
- Chang, Y., Deng, C., Dore, A.J., Zhuang, G., 2015. Human excreta as a stable and important source of atmospheric ammonia in the megacity of Shanghai. *PLoS One* 10, e0144661.
- Chang, Y., Liu, X., Deng, C., Dore, A.J., Zhuang, G., 2016. Source apportionment of atmospheric ammonia before, during, and after the 2014 APEC summit in Beijing using stable nitrogen isotope signatures. *Atmos. Chem. Phys.* 16, 11635–11647.
- Chang, Y., Zou, Z., Zhang, Y., Deng, C., Hu, J., Shi, Z., Dore, A.J., Collett Jr., J.L., 2019. Assessing contributions of agricultural and nonagricultural emissions to atmospheric ammonia in a Chinese megacity. *Environ. Sci. Technol.* 53, 1822–1833.
- Chen, X., Cui, Z., Vitousek, P.M., Cassman, K.G., Matson, P.A., Bai, J., Meng, Q., Hou, P., Yue, S., Römhild, V., Zhang, F., 2011. Integrated soil–crop system management for food security. *Proc. Natl. Acad. Sci.* 108, 6399–6404.
- Chen, J., Cheng, M., Krol, M., de Vries, W., Zhu, Q., Liu, X., Zhang, F., Xu, W., 2023. Trends in anthropogenic ammonia emissions in China since 1980: a review of approaches and estimations. *Front. Environ. Sci.* 11.
- Christensen, B.T., Olesen, J.E., Sommer, S.G., 1991. Effects of temperature, wind speed and air humidity on ammonia volatilization from surface applied cattle slurry. *J. Agric. Sci.* 117, 91–100.
- Dewes, T., 2009. Effect of pH, temperature, amount of litter and storage density on ammonia emissions from stable manure. *J. Agric. Sci.* 127, 501–509.
- Feng, S., Xu, W., Cheng, M., Ma, Y., Wu, L., Kang, J., Wang, K., Tang, A., Collett, J.L., Fang, Y., Goulding, K., Liu, X., Zhang, F., 2022. Overlooked nonagricultural and wintertime agricultural NH₃ emissions in Quzhou county, North China Plain: evidence from ¹⁵N-stable isotopes. *Environ. Sci. Technol. Lett.* 9, 127–133.
- Fleming, Z.L., Monks, P.S., Manning, A.J., 2012. Review: untangling the influence of air-mass history in interpreting observed atmospheric composition. *Atmos. Res.* 104–105, 1–39.
- Fu, X., Wang, S., Xing, J., Zhang, X., Wang, T., Hao, J., 2017. Increasing ammonia concentrations reduce the effectiveness of particle pollution control achieved via SO₂ and NO_x emissions reduction in East China. *Environ. Sci. Technol. Lett.* 4, 221–227.
- Giannadaki, D., Giannakis, E., Pozzer, A., Lelieveld, J., 2018. Estimating health and economic benefits of reductions in air pollution from agriculture. *Sci. Total Environ.* 622–623, 1304–1316.
- Gu, M., Pan, Y., Sun, Q., Walters, W.W., Song, L., Fang, Y., 2022a. Is fertilization the dominant source of ammonia in the urban atmosphere? *Sci. Total Environ.* 838, 155890.
- Gu, M., Pan, Y., Walters, W.W., Sun, Q., Song, L., Wang, Y., Xue, Y., Fang, Y., 2022b. Vehicular emissions enhanced ammonia concentrations in winter mornings: insights from diurnal nitrogen isotopic signatures. *Environ. Sci. Technol.* 56, 1578–1585.
- Gunthe, S.S., Liu, P., Panda, U., Raj, S.S., Sharma, A., Darbyshire, E., Reyes-Villegas, E., Allan, J., Chen, Y., Wang, X., Song, S., Pöhlker, M.L., Shi, L., Wang, Y., Kommula, S. M., Liu, T., Ravikrishna, R., McFiggans, G., Mickley, L.J., Martin, S.T., Pöschl, U., Andreae, M.O., Coe, H., 2021. Enhanced aerosol particle growth sustained by high continental chlorine emission in India. *Nat. Geosci.* 14, 77–84.
- Han, X., Zhu, L., Liu, M., Song, Y., Zhang, M., 2020. Numerical analysis of agricultural emissions impacts on PM_{2.5} in China using a high-resolution ammonia emission inventory. *Atmos. Chem. Phys.* 20, 9979–9996.
- Hou, Y., Bai, Z., Lesschen, J.P., Staritsky, I.G., Sikirica, N., Ma, L., Velthof, G.L., Oenema, O., 2016. Feed use and nitrogen excretion of livestock in EU-27. *Agr. Ecosyst Environ.* 218, 232–244.
- Hu, Q., Zhang, L., Evans, G.J., Yao, X., 2014. Variability of atmospheric ammonia related to potential emission sources in downtown Toronto, Canada. *Atmos. Environ.* 99, 365–373.
- Huang, X., Song, Y., Li, M., Li, J., Huo, Q., Cai, X., Zhu, T., Hu, M., Zhang, H., 2012. A high-resolution ammonia emission inventory in China. *Global Biogeochem. Cycles* 26, n/a–n/a.
- Huang, S., Lv, W., Bloszies, S., Shi, Q., Pan, X., Zeng, Y., 2016. Effects of fertilizer management practices on yield-scaled ammonia emissions from croplands in China: a meta-analysis. *Field Crop Res.* 192, 118–125.
- Ju, X., Zhang, C., 2017. Nitrogen cycling and environmental impacts in upland agricultural soils in North China: a review. *J. Integr. Agric.* 16, 2848–2862.
- Kang, Y., Liu, M., Song, Y., Huang, X., Yao, H., Cai, X., Zhang, H., Kang, L., Liu, X., Yan, X., He, H., Zhang, Q., Shao, M., Zhu, T., 2016. High-resolution ammonia emissions inventories in China from 1980 to 2012. *Atmos. Chem. Phys.* 16, 2043–2058.
- Kang, J., Wang, J., Heal, M.R., Goulding, K., de Vries, W., Zhao, Y., Feng, S., Zhang, X., Gu, B., Niu, X., Zhang, H., Liu, X., Cui, Z., Zhang, F., Xu, W., 2023. Ammonia mitigation campaign with smallholder farmers improves air quality while ensuring high cereal production. *Nat. Food* 4, 751–761.
- Kawashima, H., Kurahashi, T., 2011. Inorganic ion and nitrogen isotopic compositions of atmospheric aerosols at Yurihonjo, Japan: implications for nitrogen sources. *Atmos. Environ.* 45, 6309–6316.
- LaGro, J.A., 2005. Land-use classification. In: Hillel, D. (Ed.), *Encyclopedia of Soils in the Environment*. Elsevier, Oxford, pp. 321–328.

- Lan, Z., Lin, W., Pu, W., Ma, Z., 2021. Measurement report: exploring NH_3 behavior in urban and suburban Beijing: comparison and implications. *Atmos. Chem. Phys.* 21, 4561–4573.
- Liu, D., Fang, Y., Tu, Y., Pan, Y., 2014. Chemical method for nitrogen isotopic analysis of ammonium at natural abundance. *Anal. Chem.* 86, 3787–3792.
- Liu, X., Xiao, H., Xiao, H., Song, W., Sun, X., Zheng, X., Liu, C., Koba, K., 2017. Stable isotope analyses of precipitation nitrogen sources in Guiyang, southwestern China. *Environ. Pollut.* 230, 486–494.
- Liu, L., Xu, W., Lu, X., Zhong, B., Guo, Y., Lu, X., Zhao, Y., He, W., Wang, S., Zhang, X., Liu, X., Vitousek, P., 2022. Exploring global changes in agricultural ammonia emissions and their contribution to nitrogen deposition since 1980. *Proc. Natl. Acad. Sci.* 119, e2121998119.
- Louie, P.K.K., Chow, J.C., Chen, L.W.A., Watson, J.G., Leung, G., Sin, D.W.M., 2005. $\text{PM}_{2.5}$ chemical composition in Hong Kong: urban and regional variations. *Sci. Total Environ.* 338, 267–281.
- Ma, L., Ma, W.Q., Velthof, G.L., Wang, F.H., Qin, W., Zhang, F.S., Oenema, O., 2010. Modeling nutrient flows in the food chain of China. *J. Environ. Qual.* 39, 1279–1289.
- Meng, Z.Y., Lin, W.L., Jiang, X.M., Yan, P., Wang, Y., Zhang, Y.M., Jia, X.F., Yu, X.L., 2011. Characteristics of atmospheric ammonia over Beijing, China. *Atmos. Chem. Phys.* 11, 6139–6151.
- Meng, F., Wang, M., Strokal, M., Kroese, C., Ma, L., Li, Y., Zhang, Q., Wei, Z., Hou, Y., Liu, X., Xu, W., Zhang, F., 2022a. Nitrogen losses from food production in the North China Plain: a case study for Quzhou. *Sci. Total Environ.* 816.
- Meng, F., Zhang, Y., Kang, J., Heal, M.R., Reis, S., Wang, M., Liu, L., Wang, K., Yu, S., Li, P., Wei, J., Hou, Y., Zhang, Y., Liu, X., Cui, Z., Xu, W., Zhang, F., 2022b. Trends in secondary inorganic aerosol pollution in China and its responses to emission controls of precursors in wintertime. *Atmos. Chem. Phys.* 22, 6291–6308.
- Meng, F., Ronda, R., Strokal, M., Kroese, C., Ma, L., Krol, M., de Graaf, I., Zhao, Y.H., Wang, Y.T., Du, X.H., Liu, X.J., Xu, W., Zhang, F.S., Wang, M.R., 2024. Setting goals for agricultural nitrogen emission reduction to ensure safe air and groundwater quality: a case study of Quzhou, the North China Plain. *J. Environ.* 351, 119737.
- Mohankumar Saeed, E.P., Winwarter, W., Amon, B., 2018. Greenhouse gas and ammonia emissions from different stages of liquid manure management chains: abatement options and emission interactions. *J. Environ. Qual.* 47, 30–41.
- NBSC, 2021. Beijing Statistical Yearbook 2020 (in Chinese). National Bureau of Statistics of China, China Statistics Press, Beijing.
- Pan, Y., Tian, S., Liu, D., Fang, Y., Zhu, X., Zhang, Q., Zheng, B., Michalski, G., Wang, Y., 2016. Fossil fuel combustion-related emissions dominate atmospheric ammonia sources during severe haze episodes: evidence from ^{15}N -stable isotope in size-resolved aerosol ammonium. *Environ. Sci. Technol.* 50, 8049–8056.
- Parnell, A.C., Inger, R., Bearhop, S., Jackson, A.L., 2010. Source partitioning using stable isotopes: coping with too much variation. *PLoS One* 5, e9672.
- Peng, L., Ti, C., Yin, B., Dong, W., Li, M., Tao, L., Yan, X., 2024. Traceability of atmospheric ammonia in a suburban area of the Beijing-Tianjin-Hebei region. *Sci. Total Environ.* 907.
- Poliassar, A.V., Hopke, P.K., Paatero, P., Kaufmann, Y.J., Hall, D.K., Bodhaine, B.A., Dutton, E.G., Harris, J.M., 1999. The aerosol at Barrow, Alaska: long-term trends and source locations. *Atmos. Environ.* 33, 2441–2458.
- Pozzer, A., Tsimpidi, A.P., Karydis, V.A., de Meij, A., Lelieveld, J., 2017. Impact of agricultural emission reductions on fine-particulate matter and public health. *Atmos. Chem. Phys.* 17, 12813–12826.
- Ren, B., Xie, P., Xu, J., Li, A., Tian, X., Hu, Z., Huang, Y., Li, X., Zhang, Q., Ren, H., Ji, H., 2021. Use of the PSCF method to analyze the variations of potential sources and transports of NO_2 , SO_2 , and HCHO observed by MAX-DOAS in Nanjing, China during 2019. *Sci. Total Environ.* 782.
- SCPRC (the State Council of the People's Republic of China), 2013. Air Pollution Prevention and Control Action Plan. https://www.gov.cn/zwjk/2013-09/12/content_2486773.htm.
- SCPRC (the State Council of the People's Republic of China), 2018. Three-Year Action Plan for Winning the Blue Sky Defense Battle. https://www.gov.cn/zhengce/content/2018-07/03/content_5303158.htm.
- Seinfeld, S.N., J.H.P., 2006. Atmospheric Chemistry and Physics: From Air Pollution to Climate Change: Wiley Interscience: Hoboken.
- Tanner, P.A., 2007. Vehicle-related ammonia emissions in Hong Kong. *Environ. Chem. Lett.* 7, 37–40.
- Wang, Y.Q., 2014. MeteoInfo: GIS software for meteorological data visualization and analysis. *Meteorol. Appl.* 21, 360–368.
- Wang, S.X., Zhao, B., Cai, S.Y., Klimont, Z., Nielsen, C.P., Morikawa, T., Woo, J.H., Kim, Y., Fu, X., Xu, J.Y., Hao, J.M., He, K.B., 2014. Emission trends and mitigation options for air pollutants in East Asia. *Atmos. Chem. Phys.* 14, 6571–6603.
- Wang, C., Li, X., Zhang, T., Tang, A., Cui, M., Liu, X., Ma, X., Zhang, Y., Liu, X., Zheng, M., 2022a. Developing nitrogen isotopic source profiles of atmospheric Ammonia for source apportionment of Ammonia in urban Beijing. *Front. Environ. Sci.* 10.
- Wang, M., Duan, Y., Xu, W., Wang, Q., Zhang, Z., Yuan, Q., Li, X., Han, S., Tong, H., Huo, J., Chen, J., Gao, S., Wu, Z., Cui, L., Huang, Y., Xiu, G., Cao, J., Fu, Q., Lee, S., 2022b. Measurement report: characterisation and sources of the secondary organic carbon in a Chinese megacity over 5 years from 2016 to 2020. *Atmos. Chem. Phys.* 22, 12789–12802.
- Ward, E.J., Semmens, B.X., Phillips, D.L., Moore, J.W., Bouwes, N., 2011. A quantitative approach to combine sources in stable isotope mixing models. *Ecosphere* 2.
- Wu, L., Ren, H., Wang, P., Chen, J., Fang, Y., Hu, W., Ren, L., Deng, J., Song, Y., Li, J., Sun, Y., Wang, Z., Liu, C., Ying, Q., Fu, P., 2019. Aerosol ammonium in the urban boundary layer in Beijing: insights from nitrogen isotope ratios and simulations in summer 2015. *Environ. Sci. Technol. Lett.* 6, 389–395.
- Wu, L., Wang, P., Zhang, Q., Ren, H., Shi, Z., Hu, W., Chen, J., Xie, Q., Li, L., Yue, S., Wei, L., Song, L., Zhang, Y., Wang, Z., Chen, S., Wei, W., Wang, X., Zhang, Y., Kong, S., Ge, B., Yang, T., Fang, Y., Ren, L., Deng, J., Sun, Y., Wang, Z., Zhang, H., Hu, J., Liu, C.-Q., Harrison, R.M., Ying, Q., Fu, P., 2024. Dominant contribution of combustion-related ammonium during haze pollution in Beijing. *Sci. Bull.* <https://doi.org/10.1016/j.scib.2024.01.002>. In press.
- Xu, W., Luo, X.S., Pan, Y.P., Zhang, L., Tang, A.H., Shen, J.L., Zhang, Y., Li, K.H., Wu, Q., H., Yang, D.W., Zhang, Y.Y., Xue, J., Li, W.Q., Li, Q.Q., Tang, L., Lu, S.H., Liang, T., Tong, Y.A., Liu, P., Zhang, Q., Xiong, Z.Q., Shi, X.J., Wu, L.H., Shi, W.Q., Tian, K., Zhong, X.H., Shi, K., Tang, Q.Y., Zhang, L.J., Huang, J.L., He, C.E., Kuang, F.H., Zhu, B., Liu, H., Jin, X., Xin, Y.J., Shi, X.K., Du, E.Z., Dore, A.J., Tang, S., Collett, J.L., Goulding, K., Sun, Y.X., Ren, J., Zhang, F.S., Liu, X.J., 2015. Quantifying atmospheric nitrogen deposition through a nationwide monitoring network across China. *Atmos. Chem. Phys.* 15, 12345–12360.
- Xu, W., Wu, Q., Liu, X., Tang, A., Dore, A.J., Heal, M.R., 2016. Characteristics of ammonia, acid gases, and $\text{PM}_{2.5}$ for three typical land-use types in the North China Plain. *Environ. Sci. Pollut. Res.* 23, 1158–1172.
- Xu, W., Song, W., Zhang, Y., Liu, X., Zhang, L., Zhao, Y., Liu, D., Tang, A., Yang, D., Wang, D., Wen, Z., Pan, Y., Fowler, D., Collett, Erisman, J.W., Goulding, K., Li, Y., Zhang, F., 2017. Air quality improvement in a megacity: implications from 2015 Beijing Parade Blue pollution control actions. *Atmos. Chem. Phys.* 17, 31–46.
- Xu, W., Liu, X.J., Liu, L., Dore, A.J., Tang, A.H., Lu, L., Wu, Q.H., Zhang, Y.Y., Hao, T.X., Pan, Y.P., Chen, J.M., Zhang, F.S., 2019. Impact of emission controls on air quality in Beijing during APEC 2014: implications from water-soluble ions and carbonaceous aerosol in $\text{PM}_{2.5}$ and their precursors. *Atmos. Environ.* 210, 241–252.
- Xu, W., Zhao, Y., Wen, Z., Chang, Y., Pan, Y., Sun, Y., Ma, X., Sha, Z., Li, Z., Kang, J., Liu, L., Tang, A., Wang, K., Zhang, Y., Guo, Y., Zhang, L., Sheng, L., Zhang, X., Gu, B., Song, Y., Van Damme, M., Clarisse, L., Coheur, P.-F., Collett, J.L., Goulding, K., Zhang, F., He, K., Liu, X., 2022. Increasing importance of ammonia emission abatement in $\text{PM}_{2.5}$ pollution control. *Sci. Bull.* 67, 1745–1749.
- Yang, J., Liu, Y., Qin, P., Liu, A.A., 2014. A review of Beijing's vehicle registration lottery: short-term effects on vehicle growth and fuel consumption. *Energy Policy* 75, 157–166.
- Zhang, X., Wu, Y., Liu, X., Reis, S., Jin, J., Dragosits, U., Van Damme, M., Clarisse, L., Whitburn, S., Coheur, P.F., Gu, B., 2017. Ammonia emissions may be substantially underestimated in China. *Environ. Sci. Technol.* 51, 12089–12096.
- Zhang, L., Chen, Y., Zhao, Y., Henze, D.K., Zhu, L., Song, Y., Paulot, F., Liu, X., Pan, Y., Lin, Y., Huang, B., 2018a. Agricultural ammonia emissions in China: reconciling bottom-up and top-down estimates. *Atmos. Chem. Phys.* 18, 339–355.
- Zhang, Y., Tang, A., Wang, D., Wang, Q., Benedict, K., Zhang, L., Liu, D., Li, Y., Collett Jr., J.L., Sun, Y., Liu, X., 2018b. The vertical variability of ammonia in urban Beijing, China. *Atmos. Chem. Phys.* 18, 16385–16398.
- Zhang, C., Liu, S., Wu, S., Jin, S., Reis, S., Liu, H., Gu, B., 2019a. Rebuilding the linkage between livestock and cropland to mitigate agricultural pollution in China. *Resour. Conserv. Recycl.* 144, 65–73.
- Zhang, X., Zou, Y., Fan, J., Guo, H., 2019b. Usage pattern analysis of Beijing private electric vehicles based on real-world data. *Energy* 167, 1074–1085.
- Zhang, Y., Benedict, K.B., Tang, A., Sun, Y., Fang, Y., Liu, X., 2020. Persistent nonagricultural and periodic agricultural emissions dominate sources of ammonia in urban Beijing: evidence from ^{15}N stable isotope in vertical profiles. *Environ. Sci. Technol.* 54, 102–109.
- Zhang, Y., Ma, X., Tang, A., Fang, Y., Misselbrook, T., Liu, X., 2023. Source apportionment of atmospheric ammonia at 16 sites in China using a bayesian isotope mixing model based on delta $^{15}\text{N}(\text{NH}_3)$ signatures. *Environ. Sci. Technol.* 57, 6599–6608.
- Zhao, P.S., Dong, F., He, D., Zhao, X.J., Zhang, X.L., Zhang, W.Z., Yao, Q., Liu, H.Y., 2013. Characteristics of concentrations and chemical compositions for $\text{PM}_{2.5}$ in the region of Beijing, Tianjin, and Hebei, China. *Atmos. Chem. Phys.* 13, 4631–4644.
- Zheng, B., Tong, D., Li, M., Liu, F., Hong, C., Geng, G., Li, H., Li, X., Peng, L., Qi, J., Yan, L., Zhang, Y., Zhao, H., Zheng, Y., He, K., Zhang, Q., 2018. Trends in China's anthropogenic emissions since 2010 as the consequence of clean air actions. *Atmos. Chem. Phys.* 18, 14095–14111.
- Zhou, F., Ciais, P., Hayashi, K., Galloway, J., Kim, D.G., Yang, C., Li, S., Liu, B., Shang, Z., Gao, S., 2016. Re-estimating NH_3 emissions from Chinese cropland by a new nonlinear model. *Environ. Sci. Technol.* 50, 564–572.
- Zong, Z., Wang, X., Tian, C., Chen, Y., Fang, Y., Zhang, F., Li, C., Sun, J., Li, J., Zhang, G., 2017. First assessment of NO_x sources at a regional background site in north China using isotopic analysis linked with modeling. *Environ. Sci. Technol.* 51, 5923–5931.